nature materials

SUPPLEMENTARY INFORMATION

DOI: 10.1038/NMAT4821

In the format provided by the authors and unedited.

Negating interfacial impedance in garnet-based solid-state Li metal batteries

Xiaogang Han,[1,a] Yunhui Gong,[1,a] Kun (Kelvin) Fu, [1,a] Xingfeng He,[1] Gregory T. Hitz,[1] Jiaqi Dai,[1] Alex Pearse,[1] Boyang Liu,[1] Howard Wang,[1] Gary Rubloff,[1] Yifei Mo,[1] Venkataraman Thangadurai,[2] Eric D. Wachsman[1,*], Liangbing Hu[1,*]

1. University of Maryland Energy Research Center, and Department of Materials Science and Engineering, University of Maryland, College Park, Maryland 20742, USA

2. Department of Chemistry, University of Calgary, 2500 University Drive Northwest, Calgary, Alberta, Canada T2N 1N4

* Corresponding author Email: binghu@umd.edu; ewach@umd.edu

[(a)]These authors contribute equally to this work.

© 2016 Macmillan Publishers Limited, part of Springer Nature. All rights reserved.

Chemical stability test of LLCZN electrolyte with Li metal at room temperature. A shining lithium disk was punched in glovebox filled with ultrahigh pure argon gas. The disk was then completely covered with LLCZN powder followed by a long-term standing in argon (Ar) (Figure S1). After half a year, no notable change was observed on either Li metal or LLCZN powder. The lithium disk after contacting with LLCZN for such a period of time is still shining, which indicates that LLCZN is very stable existing with Li metal at room temperature.



Figure S1. (a) Freshly punched Li metal disk with a shining surface. (b) Li disk contacting LLCZN powder in glovebox filled with Ar. (c) Li metal remains shining after contacting with LLCZN for half a year.

© 2016 Macmillan Publishers Limited, part of Springer Nature. All rights reserved.

Stability test of LLCZN contacting Li metal at 300°C

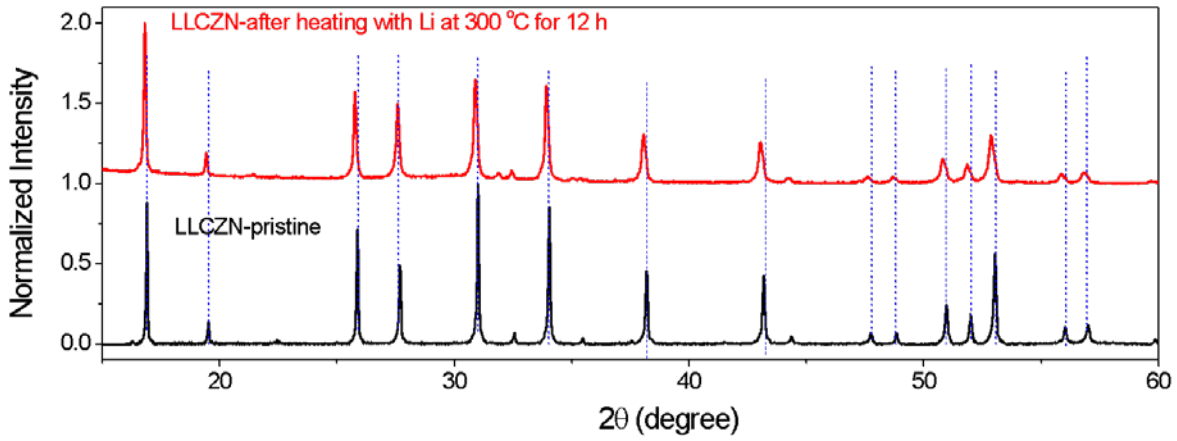


Figure S2. Shifting XRD peaks of LLCZN after heating with Li metal at 300°C for 12 hours.

© 2016 Macmillan Publishers Limited, part of Springer Nature. All rights reserved.

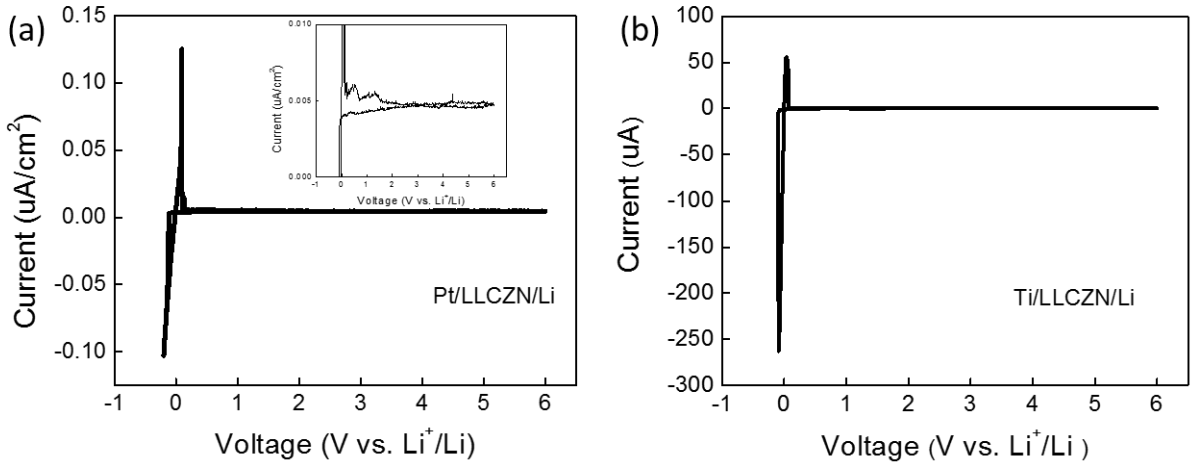


Figure S3. (a) CV curve of garnet LLCZN with Pt as working electrode and Li as reference electrode. The inset presents the zoomed-in part of the CV curve showing its non-overlap. The scan rate is 1 mV/s. (b) CV curve of garnet LLCZN with Ti as working electrode and Li as reference electrode. The voltage scan rate is 0.05 mV/s.

© 2016 Macmillan Publishers Limited, part of Springer Nature. All rights reserved.

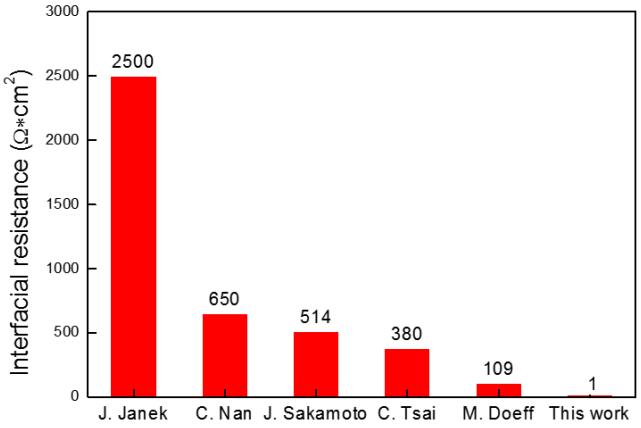


Figure S4. A comparison of interface resistances for Li/garnet from representative works and ours. The values of 1 $\Omega \cdot cm^2$ is the interfacial resistance calculated from the DC measured resistance of the symmetric cell. This value was calculated by subtracting the electrolyte resistance from the total cell resistance, dividing by two, and then normalizing to the electrode surface area. It demonstrates that the ALD-Al_2O_3 coating is effective to alleviate the main challenge of large interfacial impedance for the practical application of garnet electrolyte with Li metal anode.

Following are the reference about garnet/Li impedance:

1. Buschmann, H. *et al.* Structure and dynamics of the fast lithium ion conductor 'Li7La3Zr2O12'. *Phys. Chem. Chem. Phys.* **13,** 19378–19392 (2011).

2. Liu, T. *et al.* Achieving high capacity in bulk-type solid-state lithium ion battery based on Li6.75La3Zr1.75Ta0.25O12 electrolyte: Interfacial resistance. *J. Power Sources* **324,** 349–357 (2016).

3. Tsai, C.-L. *et al.* Li $_7$ La $_3$ Zr $_2$ O $_{12}$ Interface Modification for Li Dendrite Prevention. *ACS Appl. Mater. Interfaces* **8,** 10617–10626 (2016).

4. Cheng, L. *et al.* The origin of high electrolyte-electrode interfacial resistances in lithium cells containing garnet type solid electrolytes. *Phys. Chem. Chem. Phys.* **16,** 18294–18300 (2014).

5. Sharafi, A., Meyer, H. M., Nanda, J., Wolfenstine, J. & Sakamoto, J. Characterizing the Li-Li7La3Zr2O12 interface stability and kinetics as a function of temperature and current density. *J. Power Sources* **302,** 135–139 (2016).

© 2016 Macmillan Publishers Limited, part of Springer Nature. All rights reserved.

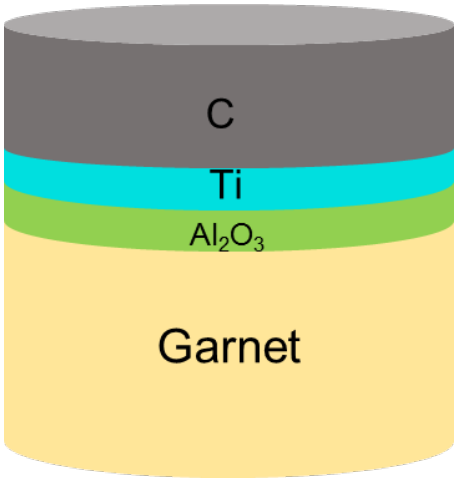


Figure S5. Illustration for the ALD-treated garnet prepared for ion milling/ or FIB/TEM sampling. The deposition of 10 nm Ti and 2 μm carbon is to protect the sample surface from damage during the sampling.

© 2016 Macmillan Publishers Limited, part of Springer Nature. All rights reserved.

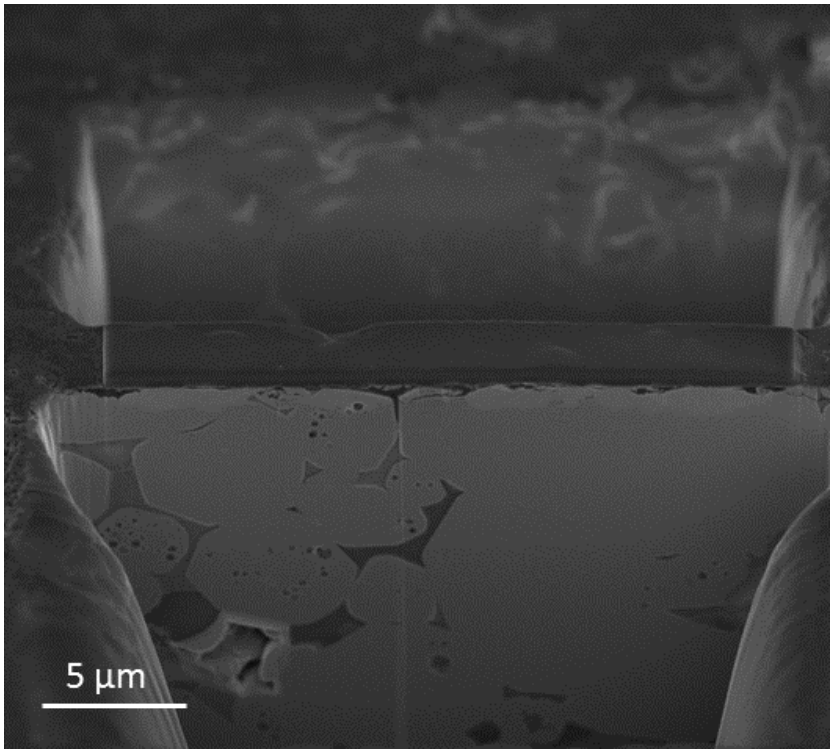


Figure S6. SEM image for FIB sample of ALD-treated garnet. Some voids can be observed.

© 2016 Macmillan Publishers Limited, part of Springer Nature. All rights reserved.

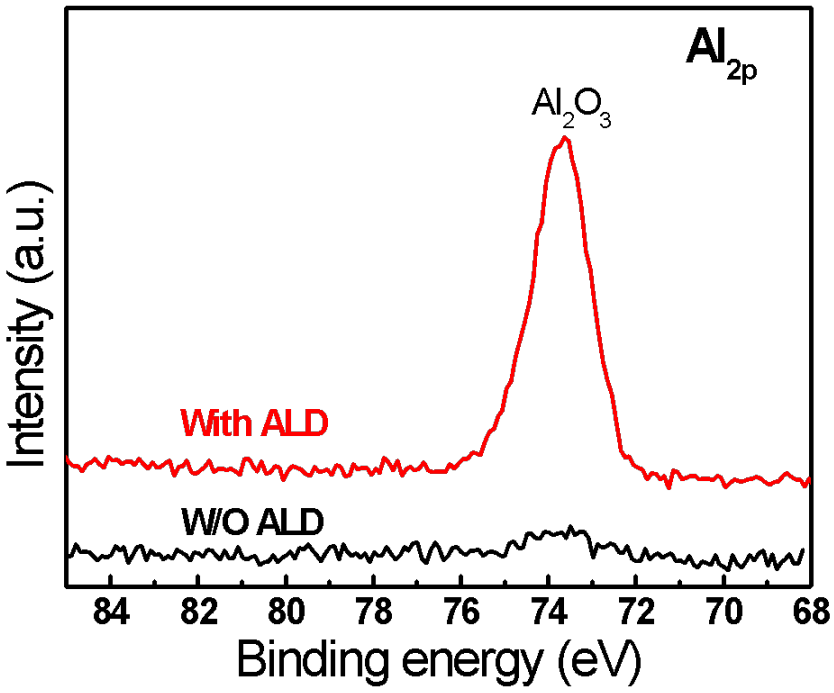


Figure S7. The comparison of C 1s peaks and the corresponding fitting curves in the XPS results for garnet solid electrolyte before and after ALD-Al_2O_3 coating.

© 2016 Macmillan Publishers Limited, part of Springer Nature. All rights reserved.

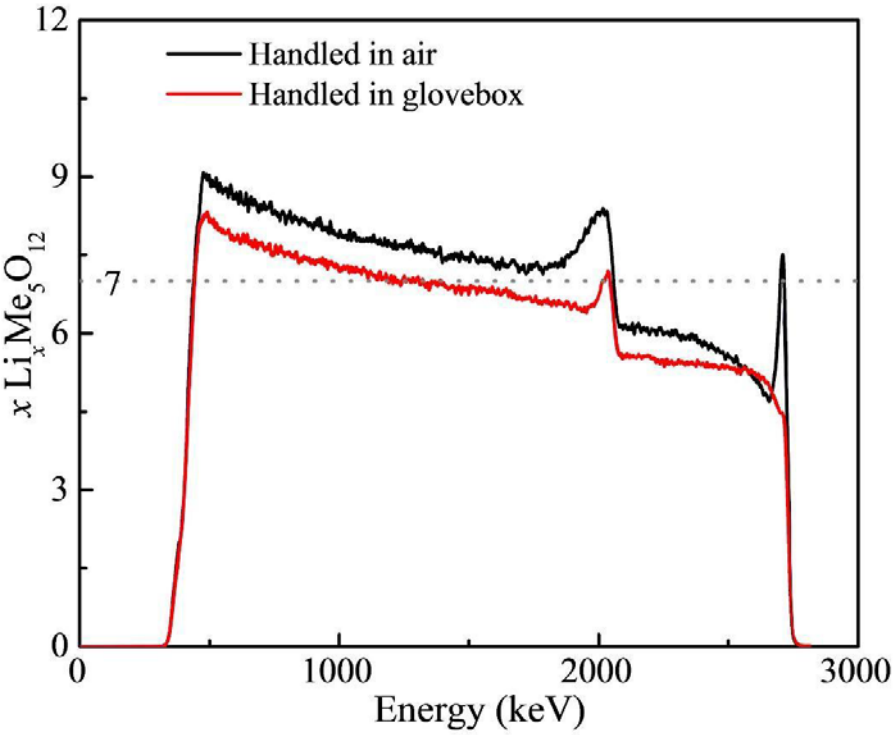
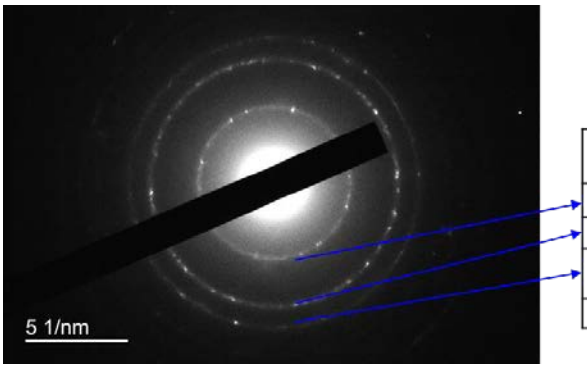


Figure S8. The effect of ALD coating on surface segregation is compared. As the specimen handed in glove box shows less surface segregation, the two specimens handled in air display similar Li segregation, with or without ALD coating of Al_2O_3 layers.

© 2016 Macmillan Publishers Limited, part of Springer Nature. All rights reserved.



Crystal symmetry

High Low

Measured d spacing (Å)	$Li_2Al_4O_7$ (Fd-3m)	$Li_2Al_4O_7$ (Fd-3m)	$LiAl_5O_8$ ($P4_332$)	$LiAl_5O_8$ ($P4_332$)	$LiAlO_2$ ($P4_12_12$)	$LiAlO_2$ ($P4_12_12$)
2.7	2.797	(220)	2.796	(002)	2.68	(102)
1.688	1.615	(224)	1.868	(323)	1.66	(031)
1.44	1.398	(404)	1.398	(404)		
ICSD #	83017		10480		23815	

Figure S9. SEAD of the part between Al_2O_3 and garnet and its composition analysis.

© 2016 Macmillan Publishers Limited, part of Springer Nature. All rights reserved.

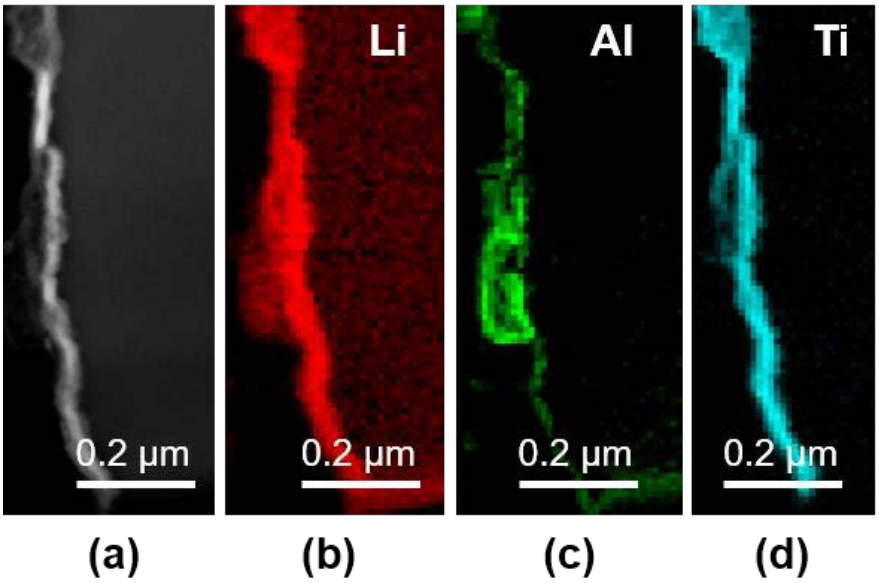


Figure S10. EELS for ALD-treated garnet with heating at 250°C for 60 min, showing Li diffusion into and through the ALD-Al_2O_3 layer. (a) HAADF image; (b-d) elemental mapping for Li, Al, and Ti.

© 2016 Macmillan Publishers Limited, part of Springer Nature. All rights reserved.

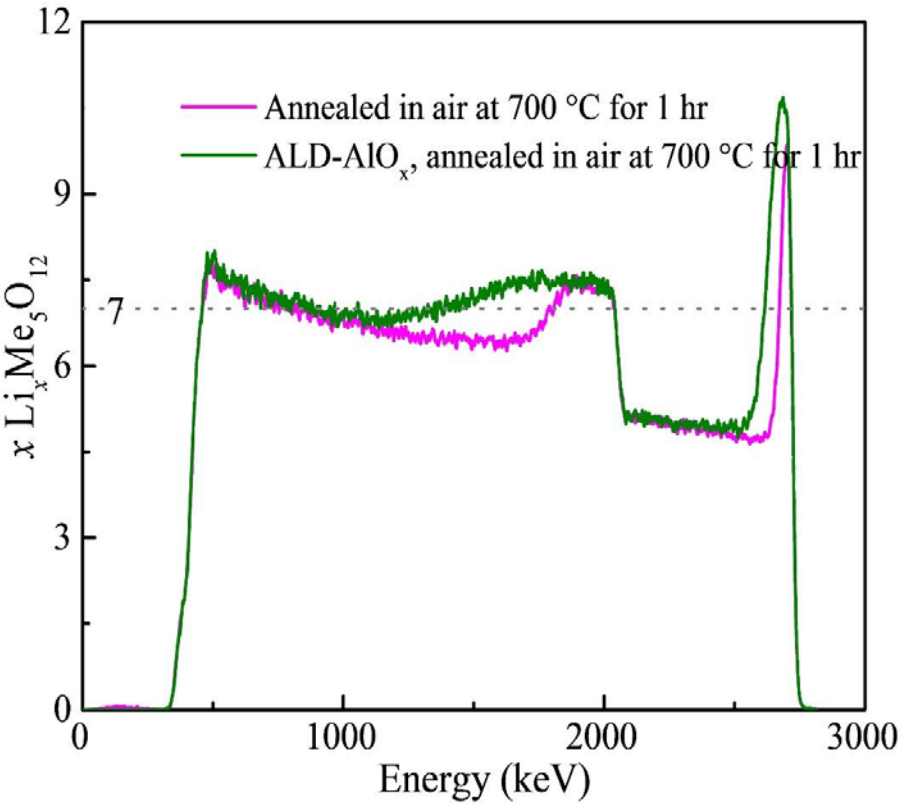


Figure S11. The effect of ALD coating on thermal annealing is compared. Significantly more Li surface excess on ALD coated specimen is observed.

© 2016 Macmillan Publishers Limited, part of Springer Nature. All rights reserved.

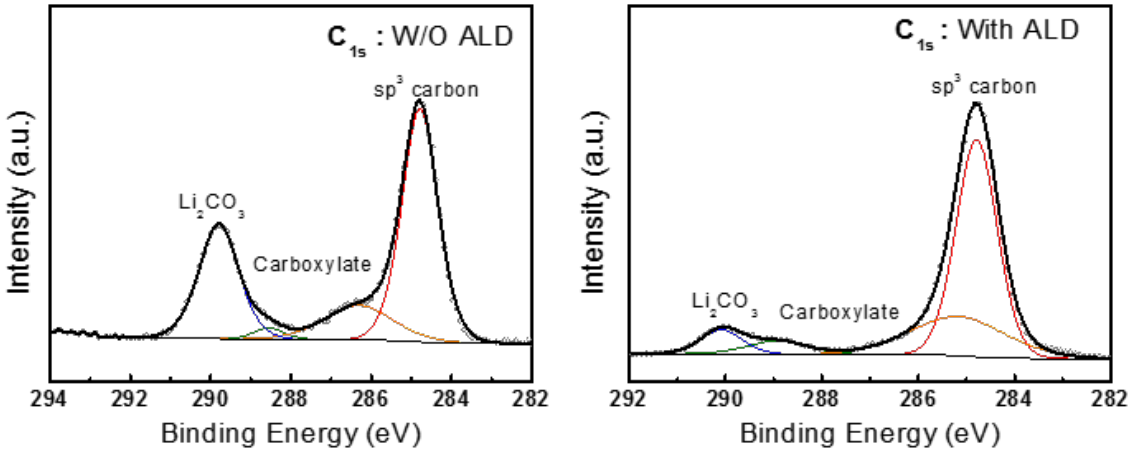


Figure S12. XPS results for garnet solid electrolyte with and without ALD- Al_2O_3 coating with survey spectra C_{1s} peaks and the corresponding fitting curves.

© 2016 Macmillan Publishers Limited, part of Springer Nature. All rights reserved.

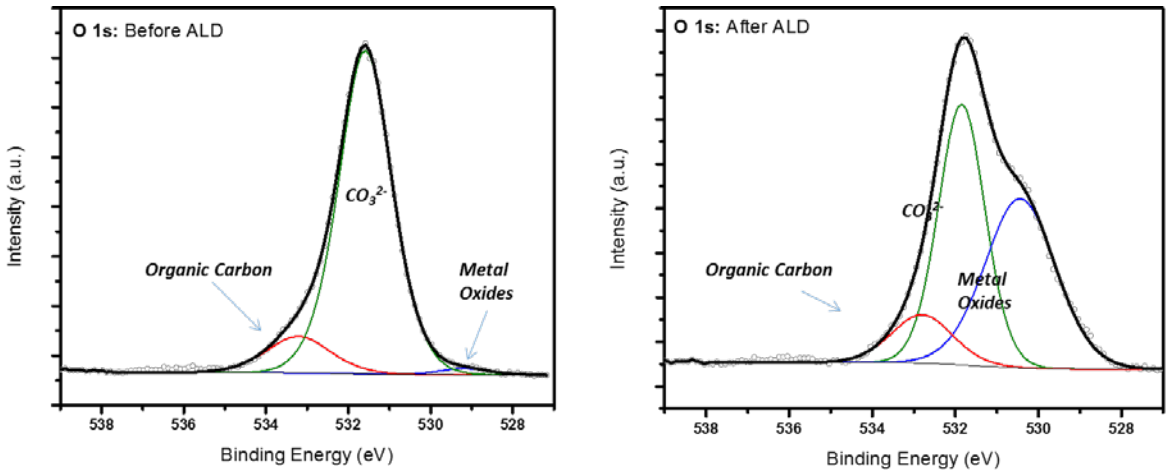


Figure S13. XPS results for garnet solid electrolyte before and after ALD-Al_2O_3 coating with survey spectra O_{1s} peaks and the corresponding fitting curves.

© 2016 Macmillan Publishers Limited, part of Springer Nature. All rights reserved.

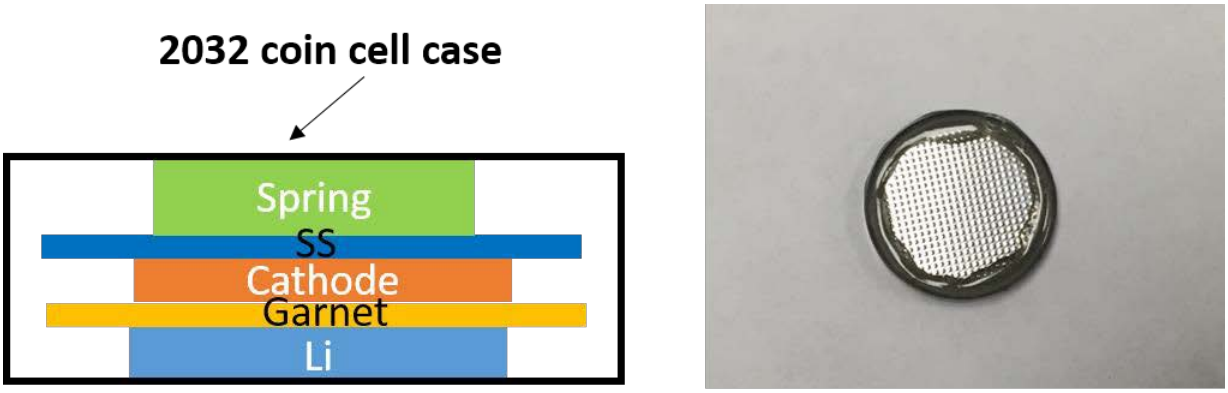


Figure S14. Schematic of a full cell sealed in a 2032 coin cell case and a photo image of a coin cell sealed by epoxy resin.

© 2016 Macmillan Publishers Limited, part of Springer Nature. All rights reserved.

First principles calculations for the stability of the LLCZN garnet materials

The materials entries for the grand potential phase diagram were obtained from the *Materials Project* database[1]. The ordering of the Li sites and the Ca/Nb dopants in the garnet structures of LLZO and LLCZN were determined using the computational methods in our prior studies.[2, 3] The configurational entropy for the Li disordering sites was included into the final energy of the garnet materials. The grand potential phase diagrams were calculated as in our prior studies[2, 3] using the pymatgen software package.[4]

First principles calculations for the binding energies of the interfaces.

The interface models comprised a slab of amorphous Li metal and a slab of the Li_2CO_3 or the lithiated alumina. The Li_2CO_3 slab had a (001) surface, which was the cleaved surface of Li_2CO_3 with the lowest surface energy. We chose the lithiated alumina of the composition $Li_xAl_2O_{3+x/2}$ (x=0.4 to 1.4) on the basis of the prior first principles calculations by Jung *et al.*[5] All the slabs with amorphous structures were prepared by a heat-and-quench method. We heated the lithiated alumina and Li metal to 2000 K and 1000 K respectively for about 4ps, and then quench them to 513K at a speed of 0.1K/fs. Finally, the amorphous structures were relaxed at 513K for 10 ps. The interface models with two slabs were equilibrated using *ab initio* molecular dynamics simulations at 513K for 30 ps. The binding energy was calculated as the energy of the interfaces minus the energy of the separated surface slabs.

© 2016 Macmillan Publishers Limited, part of Springer Nature. All rights reserved.

References

1. Jain A, Ong SP, Hautier G, Chen W, Richards WD, Dacek S*, et al.* Commentary: The Materials Project: A materials genome approach to accelerating materials innovation. *APL Materials* 2013, 1(1): 011002.

2. Mo Y, Ong SP, Ceder G. First Principles Study of the Li10GeP2S12 Lithium Super Ionic Conductor Material. *Chem Mater* 2012, 24(1): 15-17.

3. Ong SP, Mo YF, Richards WD, Miara L, Lee HS, Ceder G. Phase stability, electrochemical stability and ionic conductivity of the Li10 +/- 1MP2X12 (M = Ge, Si, Sn, Al or P, and X = O, S or Se) family of superionic conductors. *Energy & Environmental Science* 2013, 6(1): 148-156.

4. Ong SP, Richards WD, Jain A, Hautier G, Kocher M, Cholia S*, et al.* Python Materials Genomics (pymatgen): A robust, open-source python library for materials analysis. *Computational Materials Science* 2013, 68(0): 314-319.

5. Jung SC, Han Y-K. How Do Li Atoms Pass through the Al2O3 Coating Layer during Lithiation in Li-ion Batteries? *The Journal of Physical Chemistry Letters* 2013, 4(16): 2681-2685.

© 2016 Macmillan Publishers Limited, part of Springer Nature. All rights reserved.